Dynamic models of the causticizing process

ANTHONY P. SWANDA, DALE E. SEBORG, KERMIT L. HOLMAN, AND NEIL SWEERUS

ABSTRACT

Production data from a kraft mill were used to develop empirical input/output models relating key process variables to changes in production rate and lime addition. Unusually large time delays of 40–60 min in slaker and causticizer temperature measurements were attributed to sensor scaling. The data were also used to develop a physically based dynamic model containing mass and energy balances for a slaker/classifier followed by three causticizers. Parameters for the physically based dynamic model were tuned using open-loop response data from a dynamic experiment and validated using data obtained from a second dynamic experiment and during steady-state operation. The model was in excellent agreement with all collected mill data. It has been used on an industrial scale to examine process dynamics and can be used to improve causticizing process control strategies.

Application:

A model for troubleshooting or optimizing the causticizing process. Results highlight the need to clean temperature sensors frequently.

THE CAUSTICIZING PROCESS MUST effectively convert smelt from the kraft recovery boiler into a high-quality, low-variation white liquor—a caustic mixture consisting of NaOH (4.2 lb/ft^3), Na_2S (2.1 lb/ft^3), and Na_2CO_3 (0.9 lb/ft^3), all as Na_2O—for use in the mill's digesters. Production of a low-quality white liquor compromises the entire mill operation by reducing the efficiency of the digesters, the evaporators, and the recovery boiler.

Recent efforts to achieve tighter causticizer control have led to an increase in the use of advanced sensor equipment such as toroidal conductivity probes, nuclear density meters, and automatic titrators.

The literature contains few reports of dynamic models of the causticizing process. Jacobi and Williams *(1)* developed a physical dynamic model, but the model was not validated using mill data. Moreover, the dynamic response of the model to changes in key process variables was not reported. Uronen and Aurasmaa *(2)* developed dynamic, linear, empirical models (time-series models) for key process variables, but they reported only limited details about model structure and development.

This paper summarizes a study that was carried out with the objective of developing a physical dynamic model of a causticizing system. The project objectives were achieved by:

- Performing two dynamic tests on a commercial causticizing process
- Modeling the resulting process-reaction curves using first-order plus time-delay transfer functions to quantify process gains and dynamics
- Collecting and analyzing slaking and causticizing reaction-rate data
- Developing a physical dynamic model of the causticizing reactor line based on the process-reaction curves from a dynamic test
- Validating the physically based model using the data set from a second dynamic test.

The results presented in this paper address several fundamental issues missing in the literature. The dynamic model is described in full detail, and it is validated using mill production data. Moreover, the model includes physically based reaction kinetics. Finally, the dynamic characteristics of a typical causticizing process are reported.

PROCESS DESCRIPTION

The causticizing process produces caustic white liquor from green liquor, a solution mainly composed of sodium carbonate (Na_2CO_3). Causticization is a two-step process. The first step occurs primarily in a slaker, where lime is reacted with water to form calcium hydroxide, $Ca(OH)_2$. The second step occurs in the slaker-classifier and the three or four causticizers (continuously stirred tank reactors, or CSTRs), where Na_2CO_3 reacts with $Ca(OH)_2$ to form sodium hydroxide (NaOH) *(3)*. The two reactions are summarized as follows:

Slaking:

$$CaO_{(s)} + H_2O = Ca(OH)_{2(s)} \quad (1)$$

Causticizing:

$$Ca(OH)_{2(s)} + Na_2CO_{3(aq)} = CaCO_{3(s)} + 2NaOH_{(aq)} \quad (2)$$

Definitions of important terms

Many terms are used to characterize green liquor, white liquor, and the degree of reaction. The most commonly used terms are summarized in **Table I** *(4)*.

The chemical species are determined as follows:

$$[Na_2CO_3] = TTA - AA \quad (3)$$

$$[Na_2S] = 2(AA - EA) \quad (4)$$

$$NaOH] = AA - [Na_2S] \quad (5)$$

Total titratable alkali (TTA)	$[NaOH] + [Na_2CO_3] + [Na_2S] + 1/2[Na_2SO_3]$
Active alkali (AA)	$[NaOH] + [Na_2S]$
Effective alkali (EA)	$[NaOH] + 1/2[Na_2S]$
Sulfidity (S)	$100[Na_2S]/TTA$
Causticizing efficiency (%CE)	$100\{[NaOH] - [NaOH]_{GL}\} / \{[NaOH] - [NaOH]_{GL} + [Na_2CO_3]\}$
Lime availability (%A)	percentage of CaO

All concentrations are in terms of equivalent Na_2O.

I. Terms characterizing green and white liquors and the extent of reaction

	"BUMP" TESTS		STEADY-STATE TEST
Process variable	**Test I**	**Test II**	**Test III**
TTA, lb/ft^3	7.11	7.44	7.33
$[Na_2CO_3]$, lb/ft^3	4.05	4.10	4.39
Sulfidity, %	30.5	30.2	26.7
Liquor flow rate, gal/min	600	725	850
Temperature, °F	185	185	185
Green liquor, % of total			
To slaker bowl	72	72	72
To classifier	28	28	28
Lime addition rate, lb/min	281	297	346
Lime availability, %	…*	…*	88

*Not measured

II. Initial green liquor and lime process conditions for Tests I, II, and III

Equilibrium and kinetics

The objective of the causticizing process is to produce a white liquor with high causticity and a target AA. To do so, the causticizing reaction (Eq. 2) must proceed far to the right. The slaking and causticization reactions are reversible and heterogeneous, with CaO, $Ca(OH)_2$, and $CaCO_3$ being solids. Studies performed by Holman *et al. (5)* have shown the slaking reaction (Eq. 1) to be very rapid. Kojo *(6)* has determined the heat of reaction to be –65.2 kJ/mole. Theliander *(7)* determined that the causticizing reaction (Eq. 2) is slower, with an exothermic heat of reaction of –4.4 kJ/mole under normal operating conditions and –7.6 kJ/mole at infinite dilution.

Because of the exothermic nature of slaking, the forward rate increases as the temperature increases, but the maximum conversion decreases. It is also important to control the addition of lime to prevent a rapid heat rise in the slaker that would result in boil-over.

The causticizing reaction is an equilibrium reaction that proceeds to the right when lime is added to the aqueous reaction mixture. However, typical slaker aqueous solutions cannot be treated ideally to calculate equilibrium constants *(8)*. In highly concentrated kraft liquors, molar concentrations are not equal to activities, so the equilibrium constant K_c is dependent not only on temperature but also on the concentrations of the dissolved chemical species. Experiments reported by Lindberg and Ulmgren *(9)* showed that K_c depended on cation concentration and that inert ions such as HS^-, SO_4^{2-}, and Cl^- had no significant effect on K_c.

The generally accepted reaction mechanism for the conversion of calcium oxide to calcium hydroxide and then to calcium carbonate occurs at the solid–liquid interface *(8, 10)*. When calcium oxide pellets are added to the slaker, they react violently and break up into smaller particles. It is believed that the hydration front on the surface of a smaller CaO particle moves inward while simultaneously sodium carbonate reacts with the exterior $Ca(OH)_2$ and then must diffuse into the particle once the surface is covered with calcium carbonate *(8)*. Indeed, studies by Calistru *et al. (11)* showed that the internal diffusion of Na_2CO_3 was the rate-determining step in the causticizing reaction.

Theliander *(12)* evaluated a reaction-rate model assuming that the overall rate is governed by the diffusion of ions in the solid phase. The rate model is based on radial diffusion in a sphere where there is no sharp boundary between the $Ca(OH)_2$ core and $CaCO_3$ exterior *(13)*. However, the model requires knowledge of the lime particle size distribution, which limits the usefulness of the rate model, since mills never (or infrequently) measure lime particle size distributions.

The most practical kinetics studies have been reported by Holman *et al. (5)*. They developed an empiri-cal, pseudohomogeneous, kinetic model—based on work by Krishnagopalan and Dotson *(14)*—to evaluate causticizing system performance Their model, based on data from several mills, contains rate expressions and includes the effects of temperature, TTA, and lime charge. The differential form of the rate expression for the causticizing reaction is given in Eq. 6, where the subscript zero implies initial conditions.

$$dy/dt = k_1\{[Na_2CO_3]_0 (1-y)\}^3 - k_2\{[Na_2CO_3]_0 y + [EA]_0\} \quad (6)$$

Equation 6 can be transformed into an expression for the reaction rate of Na_2CO_3 by substituting $y = \{[Na_2CO_3]_0 - [Na_2CO_3]\} / [Na_2CO_3]_0$:

$$r_{Na_2CO_3} = [Na_2CO_3]_0 \{k_1[Na_2CO_3]^3 - k_2[EA]\} \quad (7)$$

Arrhenius expressions for the rate constants (k_1 and k_2) were determined at TTA = 7.02 lb/ft^3 (as Na_2O). Note that Holman *et al. (5)* found that TTA significantly affects the reaction rate, and they developed expressions linking the rate constants and TTA. Our results show that lime charges higher than what is stoichiometrically required for 100% conversion of Na_2CO_3 increased the reaction rate. Lower charges decreased the reaction rate. These findings are in agreement with the diffusion-limited reaction mechanism.

MILL EXPERIMENTS

The first step in developing a process model is to understand the static and dynamic behavior of the process. One of the best ways of gaining this insight is to disturb the process via step forcing (bump tests). Analysis of the resulting process-reaction curves (a) provides a benchmark for process gains and time constants and (b) reveals the relationship between process inputs and outputs.

To this end, a commercial causticizing process was "bumped" on June 30 and then bumped again a month later. The objectives of the tests were to:

- Analyze green-liquor variations
- Determine process gains
- Determine process time constants.

The first dynamic test was conducted by introducing a step change in green-liquor flow rate to the causticizing system while holding the lime addition rate constant. The second test was conducted by making a step change in lime addition rate while holding green-liquor flow-rate constant. These tests will be referred to as Test I and II:

- Test I: step change in green-liquor flow rate (+100 gal/min) at constant lime addition rate
- Test II: step change in lime addition rate (–29.0 lb/min) at constant green-liquor flow.

During both tests, green-liquor flow rates to the classifier and the slaker bowl, green-liquor temperature, and lime addition rate were controlled to constant setpoints. All other control loops were open. This procedure reduced the degree of undesired process disturbances and allowed all reactor temperatures and reaction rates to relax to new steady-state conditions.

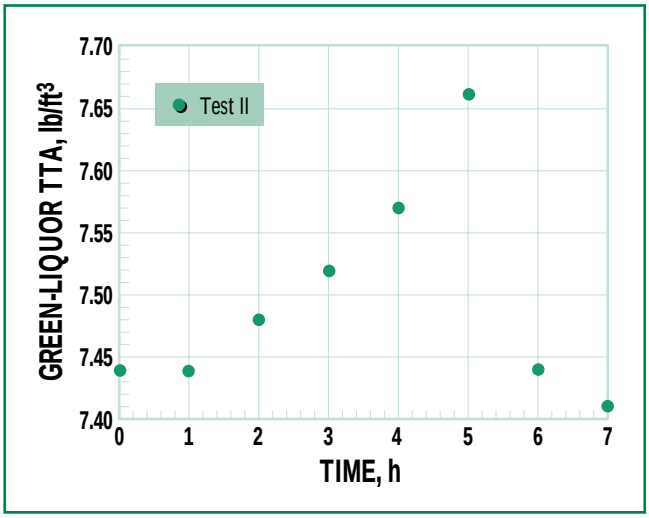

1. Variation in green-liquor TTA during Test II

Liquor samples were collected from green and white-liquor sample ports and from the top compartment of the slaker, classifier, and all causticizers. Each liquor sample sat for 5 min to allow the fine lime particles to settle. The sample was then decanted to obtain a solids-free liquor. The chemical composition of the liquors was promptly determined on-site using TAPPI Test Method T 624 cm-85 (an "ABC" test).

In addition to Tests I and II (bump tests), a set of steady-state process data was collected about six months later. This data set is referred to as Test III. Temperature was measured with a hand-held Fluke thermometer. Green- and white-liquor samples were titrated, and lime availability was measured. The errors for temperature measurements were less than ±1.0°F, and measures of [Na_2CO_3], [NaOH], and [Na_2S] were within ±0.05 lb/ft^3 (as Na_2O).

Table II shows the initial green liquor and lime process conditions for Tests I, II, and III.

Green-liquor TTA and Na_2CO_3

For the bump in green-liquor flow rate (Test I) both green-liquor TTA and Na_2CO_3 concentration were found to be constant over the 5-hour testing period. TTA time independence was determined by modeling the time dependence as a linear function and calculating a 95% confidence interval for the resulting slope. The results were that TTA = 7.13 + (0.012 ± 0.021)t, where t = time (hours). The same procedure was repeated for [Na_2CO_3] values, and the results were [Na_2CO_3] = 4.07 + (0.0014 ± 0.052)t. Because zero is included in each interval, the hypothesis that TTA and [Na_2CO_3] do not depend on time cannot be rejected.

For the bump in lime addition rate (Test II), green-liquor Na_2CO_3 concentration was again found to be constant throughout the 7-hour test, but it had a different absolute value than in Tests I and III. Using a 95% confidence interval again, Na_2CO_3 concentration dependence was 4.14 + (0.027 ± 0.074)t. However, green-liquor TTA significantly varied during the test, as shown in **Fig. 1**. TTA increased 0.2 lb/ft^3 in 4 hours and decreased the same amount in 1 hour.

Low-frequency disturbances are expected in green-liquor composition because of a large upstream clarifier. Even though the flow pattern is plug flow, the typical residence time is 8–12 hours, resulting in significant mixing via diffusion. Ramped disturbances over a 4–8-hour period are expected. The large 0.2-lb/ft^3 decrease in

	Time constant, min	Time delay, min	Deviation from initial steady state
Test I			
Temperature			
Slaker	60	40	–3.6 °F
1st causticizer	…*	…*	…*
Active alkali			
Classifier	40	0	–0.26 lb/ft^3
1st causticizer	51	0	–0.36 lb/ft^3
Test II			
Temperature			
Slaker	52	64	–2.3 °F
1st causticizer	60	60	–2.0 °F
Active alkali			
Classifier	26	3	–0.20 lb/ft^3
1st causticizer	33	6	–0.27 lb/ft^3

*1st causticizer temperature never settled to a constant value.

III. Time constants and time delays for first-order models with time delay ("bump" tests)

TTA at $t = 6$ hours is probably due to a measurement error. Also, the average TTA value was significantly higher than during Test I.

Test II illustrates the key result that both AA and %CE cannot be controlled by manipulating the lime addition rate. Although the control objective is to meet the target AA value, it is important to maintain a high %CE. Since [Na_2CO_3] did not change during Test II, the addition of lime should remain constant to maintain a constant %CE. However, white-liquor AA would then increase and decrease by approximately the same amount that the green-liquor TTA increases and decreases, 0.2 lb/ft^3. To avoid this situation, it is important to control TTA to a target value. If TTA is controlled and [Na_2S] remains constant, then both target AA and %CE values can be met by the correct addition of lime.

Transfer-function models

The objective of the bump tests was to see how the process responded to changes in the input conditions of green-liquor flow rate and lime addition rate. To this end, the process-reaction curves of slaker temperature, first-causticizer temperature, classifier AA, and first-causticizer AA were modeled as first-order plus time-delay transfer functions for both Tests I and II. The developed transfer functions are simple dynamic characterizations of the causticizing process that can be used in the development of a control system, e.g., selection of control variables based on dynamic considerations and tuning of PID-type (proportional, integral, derivative) controllers. Additional information on the development and the use of transfer-function models can be found in standard textbooks (e.g., *(15)*).

Table III lists the time constants, time delays, and deviations from the initial steady state for each variable during Tests II and III. The method used to determine the values shown in Table III is described by Swanda *(16)*. **Figures 2–5** compare the plant responses and model responses for step changes that were made at $t = 0$.

Time constants and time delays. The figures indicate that there are significant differences between the time constants and time delays of the temperature responses and the AA responses. The time constants for temperature were larger than those for AA, as seen in Table III, with time constants of 50–60 min for the slaker and about 60 min for the first causticizer. The corresponding time delays are, on average, 52 min and 60 min. The time constants for the AA responses are about two-thirds those of the temperature for Test I and about one-half for Test II, and there are essentially no time delays.

The temperature responses are slower than expected, given that the mean residence time is 25 min for the slaker and 30 min for the top compartment of the first causticizer. Because of the high scaling environment, large amounts of scale (over 4 in.) have been known to form on the temperature probes in the slaker and first causticizer. This amount of scale would drastically affect the dynamic response of temperature and, in turn, degrade the performance of any causticizing control system relying on temperature measurements.

The AA response-time constants of both tests should be approximately equal because there are essentially no flow dynamics and the reactors are approximately well-mixed slurries. However, the time constants of the AA response in the classifier and first causticizer for Test II are 14 min and 18 min less than the corresponding constants in Test I, respectively.

Process gains. Table III shows that the deviations from the initial steady states for each process variable were about the same for Tests I and II. The size of the deviation for first-causticizer AA is at the upper limit of acceptable. Typically, only ±0.2 lb/ft^3 excursions in white-liquor AA are permitted. Thus, step changes can be considered medium sized. The largest operational change in flow rate for the modeled process is 500 gal/min, and the largest possible change in lime addition rate for the examined mill is 567 lb/min. However, a 58-lb/min change would be considered large by an operator.

Unmodeled process variables. Two key variables—third causticizer AA and the white-liquor AA—could not be modeled because they did not settle to steady values in the 7-hour testing period. Determining model order and time constant(s) for white-liquor AA is important to understanding the process. The only explanation

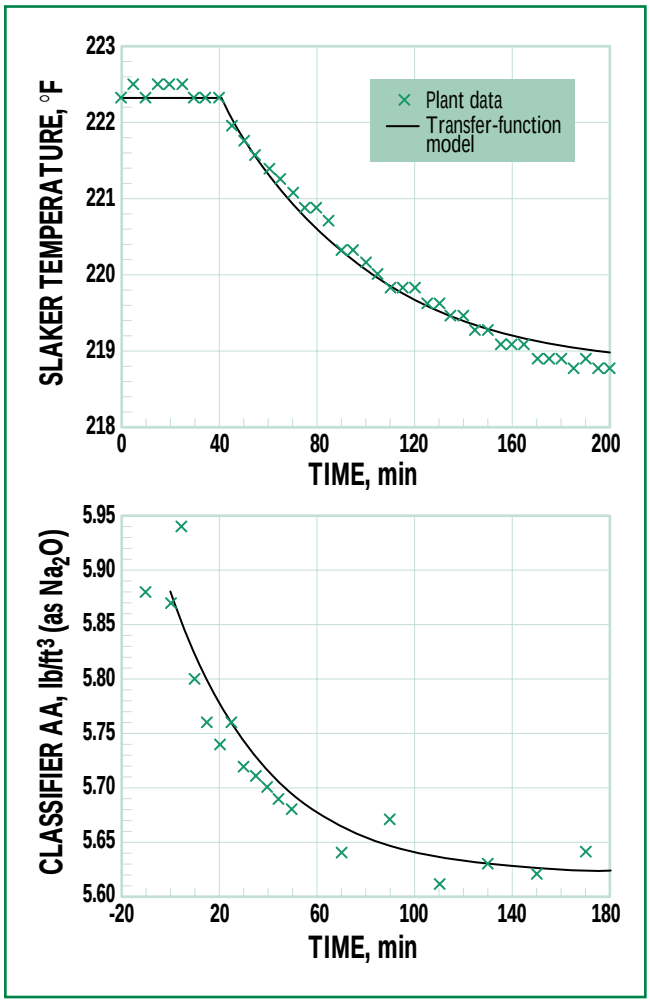

2. Predicted and actual slaker temperature and classifier AA, Test I

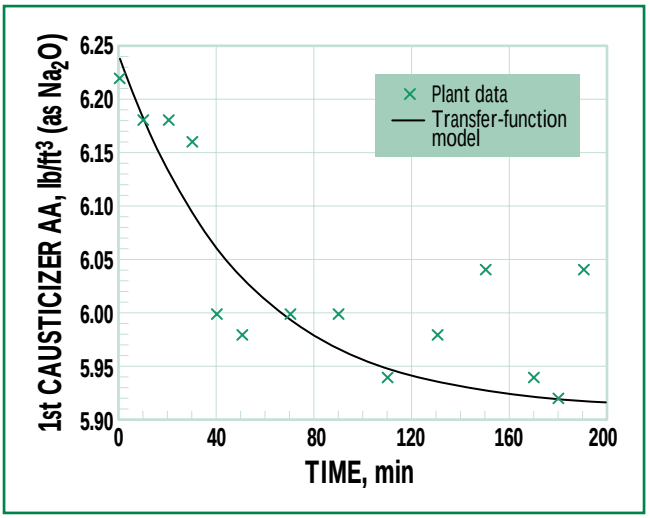

3. Predicted and actual first-causticizer AA, Test I

offered for why the settling times (the time to reach a new steady-state condition) were longer than expected in the third causticizer and white-liquor AA values is that the solids may have a slightly longer residence time than the liquid phase.

It is of critical importance to know how large an effect a step change has on white-liquor AA and causticizing efficiency. A rough estimation of the changes in AA and %CE during Test II is from 6.35 lb/ft³ to 6.05 lb/ft³ and from 77.5% to 71%, respectively. A 6.5% change in causticizing efficiency is considered very large. For Test I, the changes in AA and CE% were not estimated because these variables did not reach steady state.

DEVELOPMENT OF UNSTEADY-STATE PHYSICAL MODEL

Unsteady-state physical models provide process insight and greatly aid in the design of a control scheme. An unsteady-state physical model of the causticizing process can be used to:

- Gain a better understanding of the process
- Explore alternative operating strategies
- Evaluate slaker and causticizer performance.

The physical model also could be used to evaluate and optimize the performance of proposed causticizing control systems.

The unsteady-state physical model is based on first principles and contains only two empirical relationships. The reaction-rate expressions for the slaking and causticizing reactions were empirically modeled as pseudohomogeneous. However, both rate expressions are based on their respective physical mechanisms. Also, the model consists of energy and mass balances around the typical causticizing reactor line. Each reactor has two compartments, except for the classifier, which has only one compartment. Each compartment is defined as a control volume over which unsteady-state energy and mass balances were made. The model was tuned using Test I data and validated using data from Tests II and III.

Model assumptions for unsteady-state mass and energy balances

The physical model is constructed from a set of unsteady-state material and energy balances. Each balance is made over a reactor compartment. Two simplifying assumptions were made, namely, that both the liquid and solid particles are well mixed (i.e., they form a well-mixed slurry), and that the operating volume is constant. The assumption of a well-mixed slurry is made because work done by Holman *(17)* and Hypponen and Luuko *(18)* shows that the solids' residence-time distribution is the same as the liquor. Moreover, most mill causticizing reactors have liquor exiting via an overflow pipe, so that the liquid volume is constant.

Mass balances

Each compartmental mass balance consists of seven differential equations for seven compounds: Na_2CO_3, NaOH, Na_2S, CaO, $Ca(OH)_2$, $CaCO_3$, and solid inerts. Equations 8–10 are used to calculate the reactor exit concentrations of Na_2CO_3, NaOH, and Na_2S, respectively.

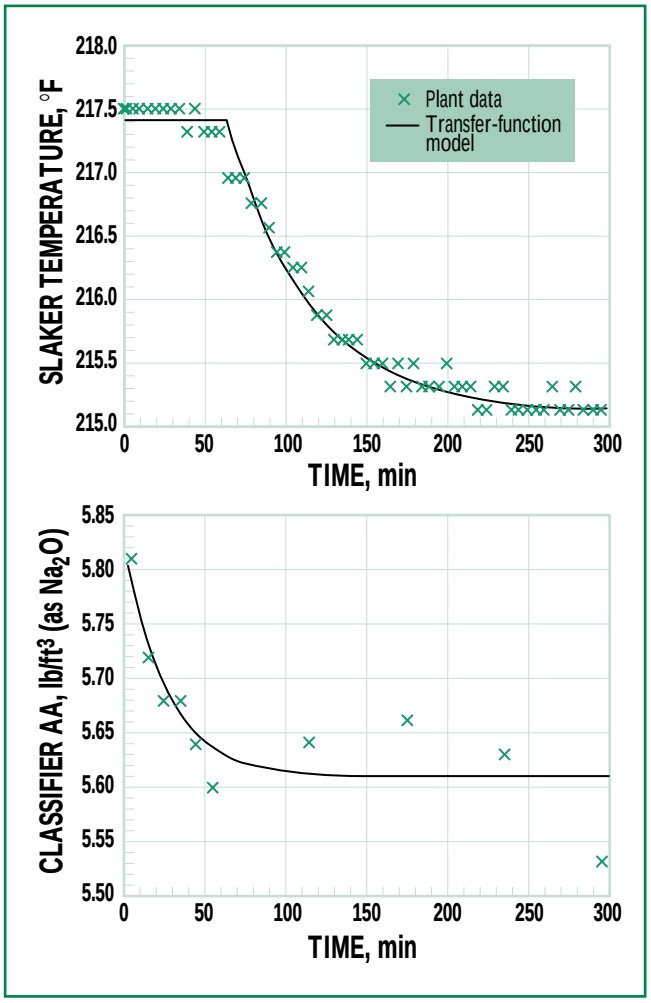

4. Predicted and actual slaker temperature and classifier AA, Test II

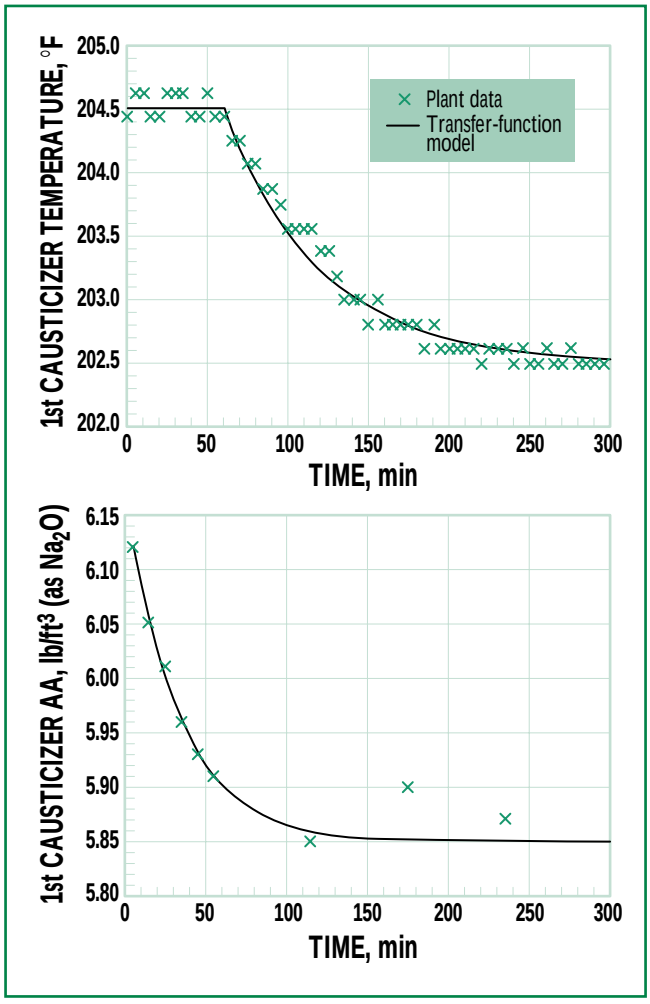

5. Predicted and actual first-causticizer temperature and AA, Test II

$$dC_a/dt = [(1/V)(q_0C_{a,0} - qC_a)] - r_a \quad (8)$$

$$dC_b/dt = [(1/V)(q_0C_{b,0} - qC_b)] + r_a \quad (9)$$

$$dC_c/dt = (1/V)(q_0C_{c,0} - qC_c) \quad (10)$$

where

C_a = concentration of Na_2CO_3 in the compartment

$C_{a,0}$ = inlet concentration of Na_2CO_3

C_b = concentration of NaOH in the compartment

$C_{b,0}$ = inlet concentration of NaOH

C_c = concentration of Na_2S in the compartment

$C_{c,0}$ = inlet concentration of Na_2S

q = volumetric flow rate, ft^3/min

q_0 = inlet volumetric flow rate, ft^3/min

r_a = causticizing reaction rate, $lb/ft^3 \cdot min$ (as Na_2O)

V = operating volume, ft^3

[Note: All concentration units are lb/ft^3 (as Na_2O).]

These three equations have the form of a standard unsteady-state mass balance for a constant-volume CSTR, except the volumetric flow rates in and out are not assumed to be equal. The outlet flow rates are less than the inlet flow rates because of water consumption by the slaking reaction.

Equation 11 is used to determine the mass of CaO present and the outlet mass flow rate of CaO for each reactor compartment. Similar calculations for $Ca(OH)_2$, $CaCO_3$, and solid inerts are determined using Eqs. 12–14, respectively. The well-mixed slurry assumption allows the exit mass flow rate of solid material to be approximated by $m_f q/V$.

$$dm_d/dt = w_{d,0} - (m_d q/V) - Vr_b \quad (11)$$

$$dm_e/dt = w_{e,0} - (m_e q/V) - V(MW_e/MW_{Na_2O})r_a + V(MW_e/MW_d)r_b \quad (12)$$

$$dm_f/dt = w_{f,0} - (m_f q/V) + V(MW_f/MW_{Na_2O})r_a \quad (13)$$

$$dm_g/dt = w_{g,0} - (m_g q/V) \quad (14)$$

where

m_d = mass of CaO in compartment, lb

m_e = mass of $Ca(OH)_2$ in compartment, lb

m_f = mass of $CaCO_3$ in compartment, lb

m_g = mass of solid inerts in compartment, lb

w = mass flow rate, lb/min

MW = molecular weight

r_b = slaking reaction rate, lb/ft^3·min.

Equation 15 is used to calculate the decrease in volumetric flow rate of green liquor, q_{GL}.

$$q_{GL} = q_{GL,0} - \{(V/\rho_{H_2O})(MW_{H_2O}/MW_{Na_2O})r_a\} \quad (15)$$

Equation 15 was derived from Eq. 16 by dividing both sides by the density of water and assuming that the accumulation term is set equal to zero.

$$dm_{H_2O}/dt = w_{H_2O,0} - w_{H_2O} - V\,(MW_{H_2O}/MW_{Na_2O})r_a \quad (16)$$

There are essentially no flow dynamics because the liquor slurry exits via an overflow pipe. Also, the increase in liquor density resulting from the increase in the concentration of dissolved ions is ignored. During nominal operations, the maximum decrease in volumetric flow rate is 2%, so that the error introduced by this approximation is insignificant.

Causticizing and slaking kinetics. The causticizing reaction rate, r_a, is calculated using Eq. 17, where $[Ca(OH)_2]_s = m_c/V$ is the "effective concentration."

$$r_{Na_2CO_3} = [Na_2CO_3]_0\,[Ca(OH)_2]_{(s)}\,\{k_1[Na_2CO_3] - k_2[EA]^2\} \quad (17)$$

Equations 18 and 19 are used to determine k_1 and k_2 at a given temperature, respectively.

$$k_{1,TTA=7.02} = k_{1,0}\exp(-11{,}700/RT) \quad (18)$$

$$k_{2,TTA=7.02} = k_{2,0}\exp(-9890/RT) \quad (19)$$

where

R = 1.987 Btu/lb·mole·°R

T = °R

E = activation energy, Btu/lb·mole

TTA = lb/ft^3 (as Na_2O)

$k_{1,0}$ = (ft^3/lb as Na_2O)(ft^3/lb$Ca(OH)_2$)/min

$k_{2,0}$ = (ft^3/lb as Na_2O)^2(ft^3/lb$Ca(OH)_2$)/min.

The values of $k_{1,0}$ and $k_{2,0}$ used in process simulations are given later in this report in Table V. The final k_1 and k_2 values are determined by Eqs. 20 and 21, respectively.

$$k_{1,TTA1}/k_{1,TTA=7.02} = \exp[-1.52(TTA_1 - 7.02)] \quad (20)$$

$$k_{2,TTA1}/k_{2,TTA=7.02} = \exp[-0.967(TTA_1 - 7.02)] \quad (21)$$

The developed reaction model was empirically determined using fractional conversion data from experiments done by Holman *et al. (5)*. They reported the reaction-rate expression given by Eq. 7. However, their model does not account for the known dependence on the type and amount of lime added ("lime charge"). To account for "lime charge," their reaction-rate model was modified in this study by multiplying Eq. 7 by $[Ca(OH)_2]_{(s)}{}^a$. The assumed form of the causticizing reaction-rate model is given by Eq. 22.

$$r_{Na_2CO_3} = [Na_2CO_3]_0\,[Ca(OH)_2]_{(s)}{}^a\,\{k_1[Na_2CO_3]^b - k_2[EA]^c\} \quad (22)$$

The numerical methods used to determine all reaction model parameters (a, b, c, $k_{1,0}$, $k_{2,0}$, and E) are discussed in Swanda *(16)*.

Based on a study by Swanda *(16)*, the slaking reaction rate was approximated by a first-order reaction-rate expression given by Eq. 23.

$$r_b = r_{CaO} = k_{slaking}\,C_{CaO} \quad (23)$$

A rate constant $k_{slaking}$ = 0.333 min^{-1} was used. The activation energy of CaO is not known, so $k_{slaking}$ was kept constant. Discrepancies between the actual reaction rate and Eq. 23 have a limited effect on the physical dynamic model because the reaction rate is essentially instantaneous compared with the residence times of the reactors.

Energy balances. The dynamic model contains an unsteady-state energy balance that accounts for enthalpy changes of all species, for both heats of reaction, and for ambient heat loss. The control volumes, for which the mass balances were made, were also used for the energy balances. Thus there are nine unsteady-state energy balances, one for each reactor compartment. Each reactor compartment is again assumed to be well mixed and to have a constant volume. Each unsteady-state energy balance consists of one differential equation, given by

$$V\rho_{slurry}C_{p,slurry}(d/dt)T = \Delta H_{liquor} + \Delta H_{solids} + (-\Delta H_{ra})Vr_a + (-\Delta H_{rb})Vr_b + UA(T_c - T_r) \quad (24)$$

where

$$\Delta H_{liquor} = C_{p,GL}\,[w_{in}(T_{in} - T_{ref}) - w_{out}(T - T_{ref})]$$

$$\Delta H_{solids} = C_{p,CaO}\,[w_{CaO,in}(T_{in} - T_{ref}) - w_{CaO,out}(T - T_{ref})] + C_{p,Ca(OH)_2}\,[w_{Ca(OH)_2,in}(T_{in} - T_{ref}) - w_{Ca(OH)_2,out}(T - T_{ref})] + C_{p,CaCO_3}\,[w_{CaCO_3,in}(T_{in} - T_{ref}) - w_{CaCO_3,out}(T - T_{ref})] + C_{p,inerts}\,[w_{inerts,in}(T_{in} - T_{ref}) - w_{inerts,out}(T - T_{ref})]$$

and where

T = reactor temperature, °F

T_{ref} = reference temperature, °F

ΔH = enthalpy change, Btu/min

$(-\Delta H)$ = heat of reaction, Btu/lb

U = overall heat-transfer coefficient, Btu/°F·min·ft^2

A = reactor surface area, ft^2

C_p = heat capacity, Btu/lb·°F

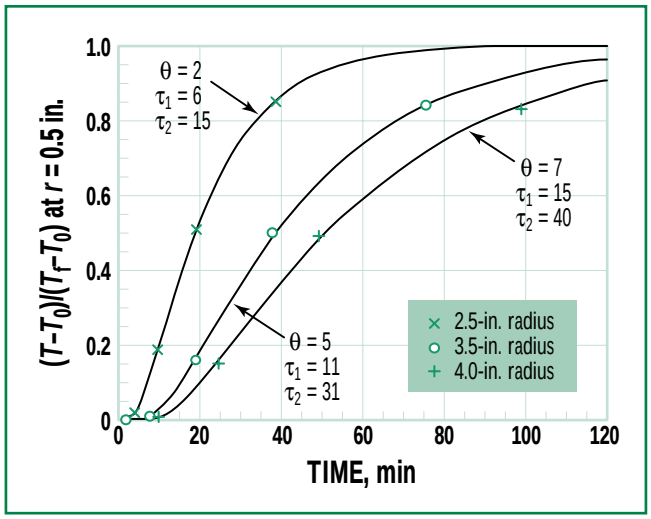

6. Dimensionless temperature response of infinite cylinders with radius 2.5 in., 3.5 in., and 4.0 in. and α = 0.027 ft²/h at r = 0.5 in.

ρ_{slurry} = slurry density, lb/ft³
w_{in} = inlet mass flow rate, lb/min
w_{out} = outlet mass flow rate, lb/min.

For simplification, all heat capacities and slurry densities are assumed constant throughout the entire reactor sequence.

The overall heat-transfer coefficient, U, was included to model the temperature decrease in the liquor as it flows through the reactor line. Its value was determined to be 2.15 Btu/°F·h·ft² using Test I data.

Temperature sensor scaling. To determine if scale could solely account for the large time delays determined earlier in this study, the dynamic effect of scaling was included in the model. The temperature probe was modeled as an infinitely long cylinder with a diameter of 1.0-in. The thermal diffusivity of the scale was assumed to be that of $CaCO_3$, $\alpha = k/\rho C_p$ = 0.027 ft²/h, where k is the thermal conductivity. During the normal operation of the causticizing process, scale as thick as 4.0 in. had been measured on temperature sensors in the slaker and first causticizer. **Figure 6** shows the dimensionless temperature response of infinitely long cylinders with radii, r, of 2.5 in., 3.5 in., and 4.0 in. and α = 0.027 ft²/h at r = 0.5 in. *(19)*. A second-order plus time-delay transfer-function model in Eq. 25 was fit to each response.

$$G(s) = \exp(-\theta s)/[(\tau_1 s+1)(\tau_2 s+1)] \qquad (25)$$

where

$G = T_m(s)/T(s)$
s = Laplace transfom variable, which is a complex variable
$T_m(s)$ = measured temperature
$T(s)$ = compartment temperature

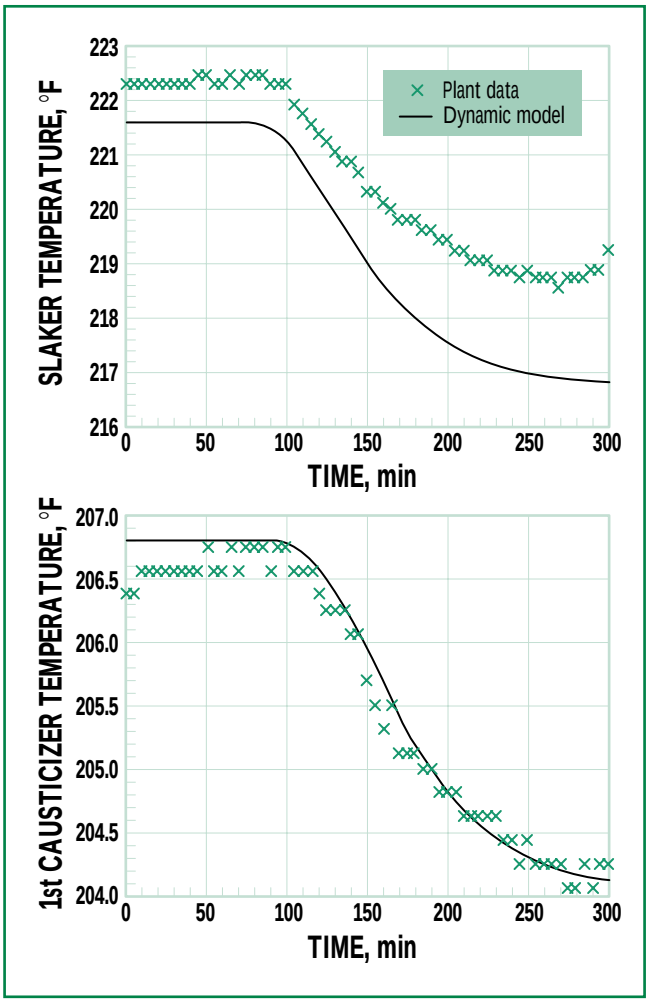

7. Predicted and actual temperatures for slaker and first causticizer, Test I

The transfer-function model parameters (θ, τ_1, τ_2) used to fit the three cylinders are shown in Fig. 6 next to the corresponding response curves.

Table IV shows the transfer-function parameters used to model the slaker and first-causticizer temperature sensor dynamics. The model parameters chosen closely represent the degree of sensor scaling observed and accurately model the plant temperature responses during Tests I and II, thus showing that scale is solely responsible for the large time delays in temperature measurements.

Model parameters. The model parameters used in simulations of Tests I, II, and III are shown in **Tables V and VI**. Four parameters were modeled as varying with the reactor compartments: volume, heat-transfer term UA, and the two preexponential factors for the rate expressions. The rate constants $k_{1,0}$ and $k_{2,0}$ were set one order of magnitude lower in the top slaker compartment than in all the other compartments, resulting in a better fit of the model to the plant data. There is also a physical justification for this modification. The lime mud particles have an average diameter between 30 μm and 45 μm within 1–2 min after being

Location	θ, min	τ_1, min	τ_2, min
Slaker	7	16	42
1st causticizer	6	13	35

IV. Transfer-function parameters used to model temperature sensor dynamics

Parameter	SLAKER COMPARTMENT Top	SLAKER COMPARTMENT Bottom	CLASSIFIER SECTION	CAUSTICIZER COMPARTMENT Top	CAUSTICIZER COMPARTMENT Bottom
Operating volume, ft³	770	1411	477	2556	2800
UA^*, Btu/°F·min	23.5	23.5	15.1	33.7	33.7
$k_{1,0}$	56.3	750	950	950	950
$k_{2,0}$	0.353	4.70	5.95	5.95	5.95

*Heat-transfer term

V. Variable parameters of the model (parameters vary with compartments)

Parameter	Value
Activation energy, Btu/lb·mole	
$E_{k,1}$	11,700
$E_{k,2}$	9,890
Heat of reaction, Btu/lb	
$\Delta H_{r,a}$, Btu/lb Na_2O	–28.6
$\Delta H_{r,b}$, Btu/lb CaO	–450
Lime availability, %	87.8
Lime temp., °F	225
$k_{slaking}$, min^{-1}	0.333
T_{ref}, °F	77
T_{atm}, °F	60
ρ_{slurry}, lb/ft³	75
Heat capacity, Btu/lb·°F	
$C_{p,GL}$	0.925
$C_{p,slurry}$	0.870
$C_{p,CaO}$	0.197
$C_{p,Ca(OH)_2}$	0.312
$C_{p,CaCO_3}$	0.225

VI. Constant parameters of the model

Location	ACTIVE ALKALI, lb/ft³ (as Na_2O) Model	Plant
Slaker		
$AA_{initial}$	5.26	5.29
AA_{final}	4.93	4.75
3rd causticizer $AA_{initial}$	6.42	6.60

VII. Comparison of Test I ("bump test") active alkali steady-state characteristics for the dynamic model and the plant data

added to the slaker. As the slaking and causticizing reactions proceed, the average diameter of the lime mud particles decreases to approximately 10–15 μm within 6–13 min later *(20)*. During this transition period, which occurs in the slaker, the reaction rate of causticizing is expected to be lower. Another possible physical justification is that some lime mud particles are short-circuiting the top slaker compartment. However, earlier tracer studies did not indicate the occurrence of any short-circuiting *(17, 18)*.

Model fitting and validation

The model was fit to the data obtained during Test I (first bump test) and then validated using data from Test II (second bump test) and Test III (steady-state operation).

Fitting of model parameters. The model was fit to data by comparing the model response to Test I response curves for slaker temperature, first-causticizer temperature, classifier AA, and first-causticizer AA. Good agreement between the model and Test I process-reaction curves was obtained by:

- Adjusting thermodynamic properties by ±10% of the initial "best guess" values
- Modeling the green-liquor split ratio between the slaker and classifier as 60%/40% instead of the 72%/28% setpoint for Tests I and II
- Modeling the green-liquor temperature as 186.5°F instead of the 185°F setpoint.

The adjustments made in thermodynamic properties and green-liquor temperature are smaller than the measurement errors. The green-liquor split ratio was lowered to raise the slaker temperature by approximately 5°F. The lower the green-liquor split ratio, the more green liquor bypasses the slaker bowl. However, the lime addition rate to the slaker bowl remains the same, so the temperature increases. Several months after Tests I and II, the measured slaker temperature dropped about 5°F when a new flow sensor for measuring green-liquor flow rate to the slaker bowl was installed. Given the previously noted adjustment in the model, it appears that the old flow element was reading higher than the actual flow rate.

Figures 7 and 8 compare modeled results with the process-reaction curves derived from plant data during Test I. (Figure 7 shows temperature in the slaker and first causticizer; Fig. 8 shows AA in the classifier and first causticizer.) Each set of reaction curves shows excellent agreement with regard to steady-state conditions, response shape, and response time. The model and process-reaction curves for first-causticizer temperature and classifier AA overlap. When the modeled first-causticizer AA process-reaction curve is shifted down by 0.04 lb/ft³, it nearly overlaps with the plant data. The only significant deviations were for the slaker temperature.

Table VII shows modeled results and Test I data for initial and final slaker AA and for initial third causticizer AA. The modeled initial and final AA in the slaker agree with the plant data. The initial AA in the third causticizer is modeled to within –0.18 lb/ft³ (as Na_2O). The maximum acceptable degree of deviation is ±0.2 lb/ft³ (as Na_2O). [The maximum acceptable deviation reflects the mill's ability to control white-liquor AA to within ±0.2 lb/ft³ (as Na_2O).]

Model validation. The dynamic model was validated by comparing modeled results with data obtained during Test II. None of the model parameters were adjusted. The only change was to set the green-liquor composition, green-liquor flow rate, and lime addition rate to match the conditions in place during Test II.

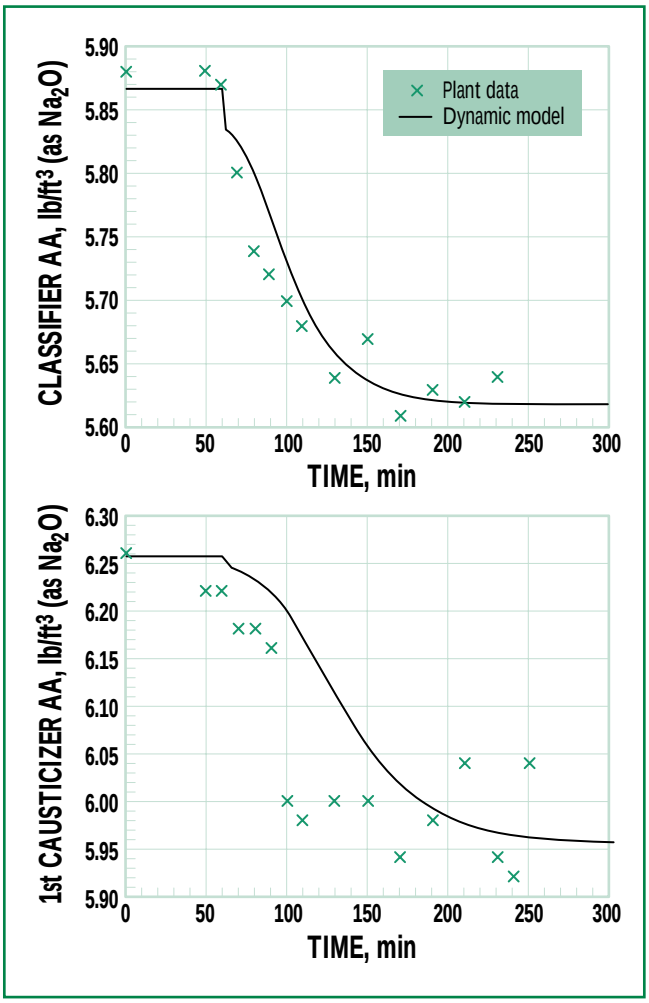

8. Predicted and actual AA for classifier and first causticizer, Test I

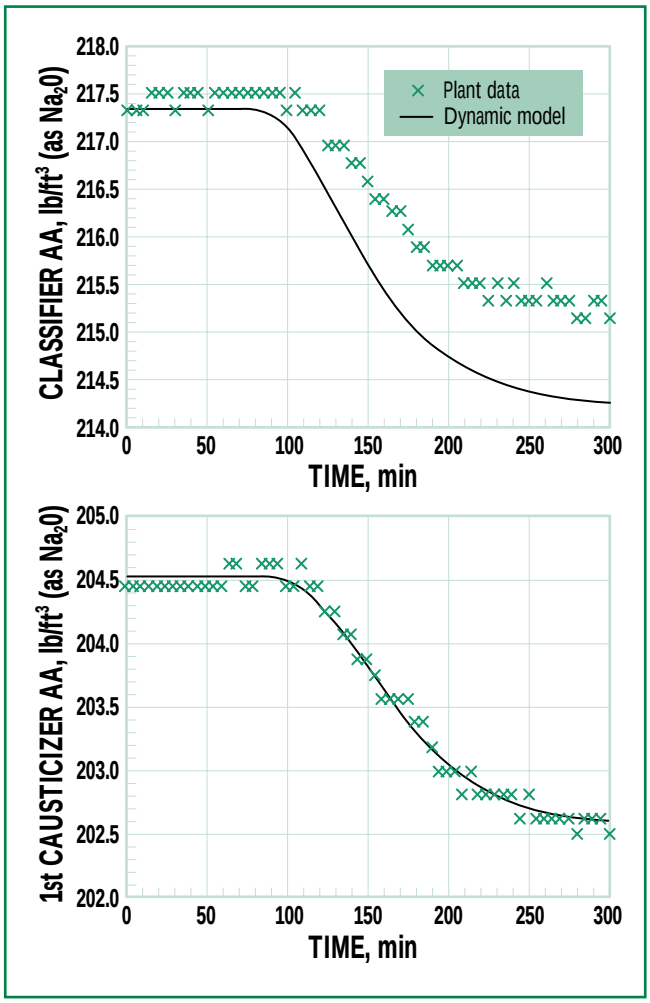

9. Predicted and actual temperatures for slaker and first causticizer, Test II

Location	ACTIVE ALKALI, lb/ft³ (as Na_2O) Model	Plant
Slaker		
$AA_{initial}$	4.88	4.86
AA_{final}	4.76	4.69
3rd causticizer $AA_{initial}$	6.30	6.22

VIII. Comparison of Test II ("bump test") active alkali steady-state characteristics for the dynamic model and the plant data

Location	Model	Plant
Slaker		
AA, lb/ft³	4.21	5.40
Temp., °F	212	214
Classifier		
AA, lb/ft³	5.58	5.63
1st causticizer		
AA, lb/ft³	5.88	6.02
Temp., °F	205	205
3rd causticizer		
AA, lb/ft³	5.99	6.07

IX. Comparison of Test III (steady state) and the dynamic model

KEYWORDS
Causticizers, causticizing, classifiers, dynamics, equations, models, performance evaluation, physical properties, process control, process variables, slakers, temperature, white liquors.

Figures 9 and 10 show comparisons for the four process-reaction curves. (Figure 9 shows temperature in the slaker and first causticizer; Fig. 10 shows AA in the classifier and first causticizer.) Again, the model accurately predicts the first-causticizer temperature curve for the process reaction and has a 30% larger gain for slaker temperature. The process-reaction curves for classifier AA have the same time-response characteristics. However, the model gain is only 65% of the plant gain. The first-causticizer AA process-reaction curve appears to lag the plant data by over 50 min. However, if the model response is rescaled using the plant gain, then the model lags by only 30 min.

Table VIII shows modeled results and Test II data for initial and final slaker AA and for initial third causticizer AA. There is excellent agreement because the model deviates from the plant data by less than 0.1 lb/ft³ (as Na_2O).

The dynamic model was also validated by comparing its output with data obtained during Test III. **Table IX** shows modeled results and Test III data for six key parameters. With the exception of slaker AA, there is excellent agreement between the modeled results and plant data.

MILL APPLICATIONS

The physically based dynamic model has been used regularly at various mills to examine process dynamics and identify equipment malfunctions. For example, after a step change in the green-liquor production rate, comparison of the process response with modeled results can help in identifying equipment malfunctions. (If an agitator malfunctions, the well-mixed CSTR approximation will not hold.) Sensor malfunctions (e.g., an extreme degree of sensor scaling) also can be identified. Besides being used to identify equipment malfunctions, the model has been used to compare the performance of different control strategies. For example, strategies to control the temperature increase between slaker input and output have been compared with strategies that control an inferred measurement of AA in one of the causticizers. Finally, the model also has been used at various mills to improve control and operation of the causticizing process.

CONCLUSIONS

The dynamic behavior of a mill causticizing system was characterized by collecting data during two "bump tests" and during steady-state operation. The resulting open-loop responses were modeled using first-order plus time-delay transfer functions. From the open-loop responses, the dynamic response of AA in the first causticizer was determined to be faster than the temperature response in the first causticizer and slaker. In addition, these temperature responses had unusually large time delays of 40–60 min, which were attributed to sensor scaling.

A physical dynamic model was developed for the continuously stirred tank reactors (CSTR) used in the causticizing process. The model parameters were fitted by using the open-loop response data of the first experiment. The model was then validated using data obtained during the second experiment and during steady-state operation.

The model was in excellent agreement with the data for both experiments. It accurately captured the steady-state characteristics of AA in the slaker, the classifier, the first causticizer, and the white liquor. The model also was in good agreement with the dynamic characteristics of AA and temperature in the classifier and first causticizer for white-liquor production rates ranging from 70% to 100% of maximum.

In an effort to obtain good agreement between the model and both experiments, substantial dynamic lag was included to account for scaling of the temperature sensors. To model this phenomenon, the scale was assumed to be 4 in. thick and to have the thermal properties of calcium carbonate. The excessive degree of scaling causes up to 60-min time delays and settling times twice as large as expected in slaker temperature measurements. Many mills with causticizing control systems use a temperature sensor in the slaker. Frequent cleaning of these sensors will minimize the dynamic lag and improve the performance of the control system. **TJ**

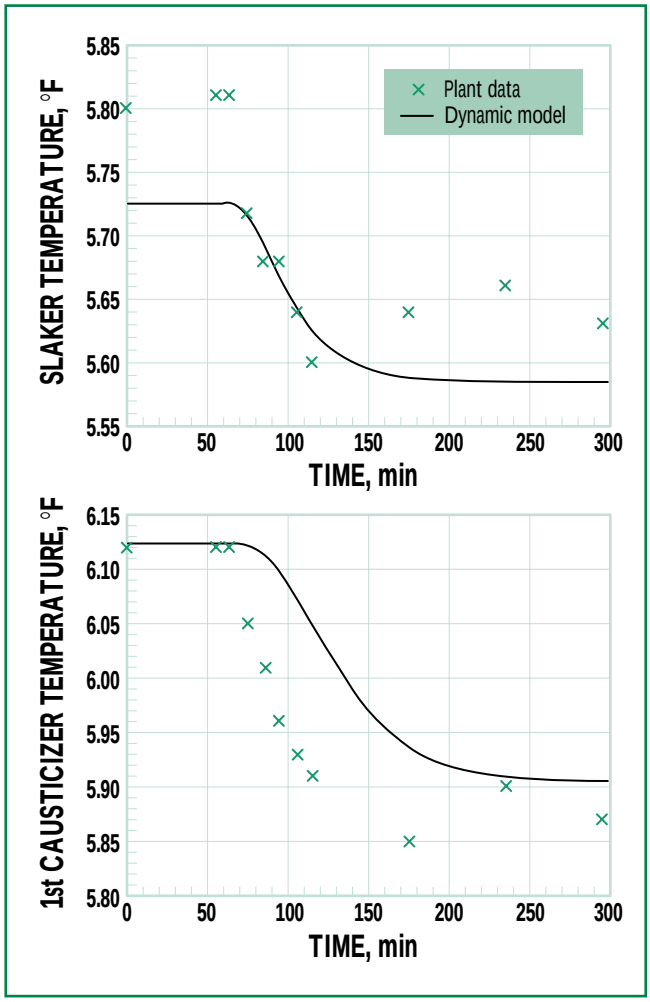

10. Predicted and actual AA for classifier and first causticizer, Test II

Swanda is a graduate student and Seborg is a professor in the Department of Chemical Engineering, University of California, Santa Barbara, CA 93106. Holman, a senior engineering specialist, and Sweerus, a systems optimization specialist, work in Process Research and Development at Weyerhaeuser Co., Tacoma, WA 98477.

Received for review Feb. 21, 1996.
Accepted Dec. 26, 1996.

LITERATURE CITED

1. Jacobi, E. F. and Williams, T. J., "A dynamic model and advanced direct digital control system for a kraft mill liquor preparation system," Vol. I: Narrative, Report 56, Purdue University, West Lafayette, IN, 1973, pp. 19–31.
2. Uronen, P. and Aurasmaa, H., *Pulp Paper Can.* 80(6): 90(1979).
3. Lavigne, J. R., *Instrumentation Applications for the Pulp and Paper Industry*, Miller Freeman, San Francisco, 1979.
4. *Chemical Recovery in the Alkaline Pulping Process* (R. P. Green and G. Hough, Eds.), TAPPI PRESS, Atlanta, 1992.
5. Holman, K. L., Warrick, R. P., and Carlson, K. R., *1991 AIChE Forest Products Symposium Proceedings*, AIChE, New York, pp. 23–31.
6. Kojo, M., *Paperi Puu* 61(8): 515(1979).
7. Theliander, H., *Nordic Pulp Paper Res. J.* 7(2): 81(1992).
8. Dorris, G. M. and Allen, L. H., *TAPPI 1988 Kraft Recovery Operations Seminar Proceedings*, TAPPI PRESS, Atlanta, pp. 31–43.
9. Lindberg, H. and Ulmgren, P., *Pulp Paper Can.* 84(3): TR7(1983).
10. Blackwell, B. B., *CPPA 72nd Annual Meeting Proceedings*, CPPA, Montreal, 1987, pp. A61–71.
11. Calistru, C., Leante, C., and Ifrin, L., *Bull. Inst. Politech. Iasi* 11: 132(1965).
12. Theliander, H., *Nordic Pulp Paper Res. J.* 3(2): 55(1988).
13. Crank, J., *The Mathematics of Diffusion*, Oxford University Press, London, 1975.
14. Krishnagopalan, A. and Dotson, B., *TAPPI 1990 Pulping Conference Proceedings*, TAPPI PRESS, Atlanta, pp. 235–44.
15. Seborg, D. E., Edgar, T. F., and Mellichamp, D. A., *Process Dynamics and Control*, John Wiley & Sons, New York, 1989.
16. Swanda, A. P., "Process modeling and control system evaluation for the pulp and paper recausticizing process," M.S. thesis, University of California, Santa Barbara, 1994.
17. Holman, K. L., "Residence time distributions in recausticizing systems," private communication, Weyerhaeuser, Tacoma, WA, 1996.
18. Hypponen, O. and Luuko, A., *Tappi J.* 67(7): 46(1984).
19. Bird, R. B., Stewart, W. E., and Lightfoot, E. N., *Transport Phenomena*, John Wiley & Sons, New York, 1960.
20. Tiljander, P. and Theliander, H., *AIChE Symp. Ser.* 92(111): 129(1996).

Statement of Ownership

1. Title of Publication: *TAPPI JOURNAL* Publication No. 07341415.
2. Date of Filing: Oct 1, 1997.
3. Frequency of Issue: Monthly. No. of Issues Published Annually: 13. Annual Subscription Price: $27.00.
4. Complete Mailing Address of Known Office of Publication: 15 Technology Parkway South, Norcross, GA 30092.
5. Complete Mailing Address of General Business Offices of the Publisher: 15 Technology Parkway South, Norcross, GA 30092.
6. Full Names and Complete Mailing Address of Publisher, Editor, and Managing Editor: TAPPI, publisher; Donald G. Meadows, Patricia M. Pauksta, and Carrie L. Reynolds, editors; Mary Beth Bennett, managing editor; all 15 Technology Parkway South, Norcross, GA 30092.
7. Owner: Technical Association of the Pulp and Paper Industry (TAPPI), 15 Technology Parkway South, Norcross, GA 30092.
8. Known Bondholders, Mortgagees, and Other Security Holders Owning or Holding 1% or more of Total Amount of Bonds, Mortgages, or Other Securities: None.
9. The purpose, function, and nonprofit status of this organization and the exempt status for Federal income tax purposes has not changed during the preceding 12 months.
10. Extent and Nature of Circulation: A. Total No. of Copies Printed: a) Average No. Copies Each Issue During Preceding 12 months—41,130; b) Actual No. Copies of Single Issue Published Nearest to Filing Date—41,673. B. Paid and/or Requested Circulation: 1) Sales Through Dealers and Carriers, Street Vendors, and Counter Sales: None; 2) Mail Subscriptions: a) Average No. Copies Each Issue During Preceding 12 Months—30,867; b) Actual No. Copies of Single Issue Published Nearest to Filing Date—30,903. C. Total Paid and/or Requested Circulation: a) Average No. Copies Each Issue During Preceding 12 Months—30,867; b) Actual No. Copies of Single Issue Published Nearest to Filing Date— 30,903. D. Free Distribution by Mail: a) Average No. Copies Each Issue During Preceding 12 Months—9,762; b) Actual No. Copies of Single Issue Published Nearest to Filing Date—9,915. E. Free Distribution Outside the Mail: None; F. Total Free Distribution: a) Average No. Copies Each Issue During Preceding 12 months—9,762; b) Actual No. Copies of Single Issue Published Nearest Filing Date—9,915; G. Total Distribution: a) Average No. Copies Each Issue During Preceding 12 Months—40,629; b) Actual No. Copies of Single Issue Published Nearest to Filing Date—40,818. H. Copies Not Distributed: 1) Office use: a) Average No. Copies Each Issue During Preceding 12 Months—501; b) Actual No. Copies of Single Issue Published Nearest to Filing Date—855. 2) Return from New Agents: None. I. Total: a) Average No. Copies Each Issue During Preceding 12 Months— 41,130; b) Actual No. Copies of Single Issue Published Nearest Filing Date—41,673.

We certify that the statements made are correct and complete.
TAPPI, Publisher